Journal of Nuclear Materials 477 (2016) 157–164

Contents lists available at ScienceDirect

Journal of Nuclear Materials

journal homepage: www.elsevier.com/locate/jnucmat

The influence of stress state on the reorientation of hydrides in a zirconium alloy

Mahmut N. Cinbiz [a, *], Donald A. Koss [b], Arthur T. Motta [a, b]

[a] Department of Mechanical and Nuclear Engineering, Pennsylvania State University, University Park, PA 16802, USA
[b] Department of Materials Science and Engineering, Pennsylvania State University, University Park, PA 16802, USA

ARTICLE INFO

Article history:
Received 17 December 2015
Received in revised form
17 April 2016
Accepted 3 May 2016
Available online 7 May 2016

Keywords:
Zirconium alloys
Hydrides
Stress state
Threshold stress
Hydride reorientation

ABSTRACT

Hydride reorientation can occur in spent nuclear fuel cladding when subjected to a tensile hoop stress above a threshold value during cooling. Because in these circumstances the cladding is under a multiaxial stress state, the effect of stress biaxiality on the threshold stress for hydride reorientation is investigated using hydrided CWSR Zircaloy-4 sheet specimens containing ~180 wt ppm of hydrogen and subjected to a two-cycle thermo-mechanical treatment. The study is based on especially designed specimens within which the stress biaxiality ratios range from uniaxial ($\sigma_2/\sigma_1 = 0$) to "near-equibiaxial" tension ($\sigma_2/\sigma_1 = 0.8$). The threshold stress is determined by mapping finite element calculations of the principal stresses and of the stress biaxiality ratio onto the hydride microstructure obtained after the thermo-mechanical treatment. The results show that the threshold stress (maximum principal stress) decreases from 155 to 75 MPa as the stress biaxiality increases from uniaxial to "near-equibiaxial" tension.

1. Introduction

Zirconium-based alloys have been widely used in the nuclear industry as nuclear fuel cladding in nuclear power reactors because of their low neutron absorption cross-section, high temperature corrosion resistance and adequate mechanical properties. However, as a byproduct of waterside corrosion, hydrogen is picked-up by the cladding. While up to 120 wt ppm of hydrogen can typically be in solution in a zirconium alloy during elevated temperature operation [1,2], when the reactor shuts down and the cladding cools, nearly all of the hydrogen precipitates as "in-plane" (circumferential) zirconium hydride platelets, especially when the material is in the cold worked and stress relieved (CWSR) condition. Upon removal of the rods from the spent fuel pool for placement in dry storage, there is a concern that the drying operations, which consist of heating the rods to high temperature, could cause hydrides to dissolve and reprecipitate in a reoriented direction as "out-of-plane" (radial) hydrides with platelet faces parallel to the hoop direction of the cladding tube. This phenomenon has been known for a long time; that is, when cooled under a sufficiently high applied stress the dissolved hydrogen can precipitate as reoriented hydrides perpendicular to the applied stress[1] [3–5]. The occurrence of hydride reorientation depends on the external stress applied to the cladding caused by the initial fill gas and gaseous fission products in the spent nuclear fuel rod.

Although hydride reorientation is influenced by properties inherent to the alloy such as the degree of cold work, grain microstructure, texture, and others [5–10], and by parameters related to the specific thermo-mechanical treatments, such as maximum temperature, dwell time at maximum temperature, cooling rate, and number of thermo-mechanical cycles, the critical parameter is the threshold stress (σ_{th}) [11–18]. Most of the data on the threshold stress for hydride reorientation in zirconium-base alloys available in the literature has been obtained from uniaxial tension tests [6–8,16–24]. However, during the vacuum drying process, the thin-wall nuclear fuel cladding tubes are subjected to internal gas pressure and/or pellet clad mechanical interaction (PCMI) that create stress biaxiality ratios ($\sigma_2/\sigma_1 \geq 0.5$, much higher than that for uniaxial tension ($\sigma_2/\sigma_1 = 0$) [25]. Although the data are

* Corresponding author. 128 Hammond, University Park, PA 16802, USA.
E-mail addresses: mnc5109@psu.edu, mahmutcinbiz@gmail.com (M.N. Cinbiz), koss@ems.psu.edu (D.A. Koss), atm2@psu.edu (A.T. Motta).

[1] In the literature, various definitions have been employed to define the external stress to cause hydride reroeintation. The definitions in this study are given in the experimental and computational procedures section of this paper, see pages 12 and 13.

http://dx.doi.org/10.1016/j.jnucmat.2016.05.013
0022-3115/

available from studies using internally-pressurized tubes [12,13,15] that induce stress states similar to vacuum-drying, no systematic study of the effect of stress state on the threshold stress has been performed. Existing data does suggest that there may be an effect of stress state on the threshold stress for hydride reorientation. For example, data from unirradiated, cold worked and stress relieved (CWSR) Zircaloy-4 shows higher threshold stress values under uniaxial tension ($140 < \sigma_{th} < 200$ MPa) than under biaxial stress state ($\sigma_2/\sigma_1 = 0.5$) when $20 < \sigma_{th} < 115$ MPa [11,13,15,19,20,23,24].

The purpose of this study is to systematically examine and quantify the role of stress state on hydride reorientation. In this work the threshold stress to reorient hydrides is determined using specifically designed test specimens that induce stress states ranging from uniaxial tension ($\sigma_2/\sigma_1 = 0$) to near-equibiaxial tension ($\sigma_2/\sigma_1 = 0.8$). The threshold stress is obtained in each case by matching the stress states calculated by finite element analysis of the test specimens under load to the hydride microstructures (and specifically the presence of reoriented hydrides) at that specific location. The study uses Zircaloy-4 sheet containing nominally ≈180 wt ppm hydrogen as a model material subjected to identical two-cycle thermo-mechanical treatments that bound conditions of vacuum drying of spent nuclear fuel. The data thus obtained isolates the stress state effect from other parameters that may affect hydride reorientation.

2. Experimental and computational procedures

Because of experimental advantages of the use of a flat sheet compared to thin-wall tube, this study utilized flat 0.67 mm thick Zircaloy-4 sheet obtained from Teledyne Wah-Chang in the cold-worked stress relieved (CWSR) condition. As described elsewhere [26], the CWSR Zircaloy-4 sheet exhibited a strong crystallographic texture. Importantly, the Kearns factors [3] of the CWSR sheet ($f_N = 0.59$, $f_R = 0.05$, and $f_T = 0.31$ in the normal, longitudinal/rolling, and transverse directions of the sheet, respectively) are similar to those reported for unirradiated CWSR Zircaloy-4 cladding tubes (0.58, 0.10, and 0.32, respectively) [27], where the hoop direction of the tube corresponds to the orientation transverse to the rolling direction of the sheet. Therefore, the texture of the Zircaloy-4 sheets used in this study is similar to the typical texture of Zircaloy-4 cladding tubes [28], i.e., the basal planes tend to align with their poles inclined approximately ± 30° away from the normal of the tube surface and oriented toward the transverse direction [29].

The stress-relieving and hydrogen gas charging operations were conducted simultaneously in the following manner. Prior to hydrogen charging, the native oxide layer was removed from the surface using an acid solution, and the specimen was then coated with a 200 nm thick nickel layer to forestall the reformation of oxides that would impede hydrogen ingress. The specimen was put into a quartz tube furnace to which a controlled amount of hydrogen-argon gas mixture (12.5% H_2 and 87.5% Ar) was subsequently introduced into the chamber (initially at a pressure of less than 13.3 μPa) containing the cold-worked (CW) specimen at 500 °C. The temperature of the chamber was maintained for 2 h to simultaneously induce stress relief, hydrogen absorption, and the homogenizing of the hydrogen distribution throughout the sample thickness. After completion of stress anneal and hydrogen charging, the specimens were slowly furnace-cooled to 25 °C. The hydrogen concentration of each sample was determined using hot vacuum extraction by Luvak Inc. The Zircaloy-4 specimens in this study were hydrogen charged to approximately 180 wt ppm. (max. 197 wt ppm and min 157 wt ppm). This hydrogen content was chosen so that on the one hand it was sufficiently low that the hydrides present at low temperature completely dissolved at high temperature and on the other hand high enough to cause hydride precipitation at a high enough temperature where the hydrogen was sufficiently mobile.

The tensile properties of the CSWR Zircaloy-4 sheet were obtained by performing tensile tests at temperatures in the range of 25–450 °C. The mechanical response of the Zircaloy-4 sheet after it plastically yields was modeled by power law hardening; the flow parameters were determined from uniaxial tension sample experiments and from studies performed previously using similar materials [18,26,28,30–34]. The strain-hardening exponent of the sheet used in this study ($n = d\ln\sigma/d\ln\varepsilon = 0.014$ at 25 °C, 0.023 at 300 °C, and 0.022 at 400 °C) is significantly smaller than that of standard cladding ($n \cong 0.06$ at 300 °C) [31]. In fact, the strain hardening behavior of this CWSR sheet material is similar to that of irradiated cladding [35].

Three types of test specimens were designed and used to determine the effect of stress state on hydride reorientation: (1) tapered uniaxial tension, (2) “plane-strain” tension [31], and (3) “near-equibiaxial” tension specimens, As shown in Fig. 1, these samples were used to determine the threshold stresses for the onset of “out-of-plane” (radial) hydride precipitation or hydride reorientation. To simulate the hydride reorientation threshold stress for spent nuclear fuel cladding, Zircaloy-4 sheet tensile specimens were machined with the load axis along their long-transverse direction which corresponds to the circumferential (or hoop) direction of nuclear fuel cladding tubes.

Finite element analyses were performed to determine the stress state distributions within the gauge sections of the double-edge notched (“plane-strain” and “near-equibiaxial” tension) samples. Because of the small thickness of the sheet material, two-dimensional finite element computations were performed under the assumptions of (i) plane stress through the specimen thickness, (ii) specimen plastic deformation (if it occurred) with flow behavior at ~400 °C (close to the onset of hydride precipitation), and (iii) isotropic mechanical properties obtained in MATPRO [35].

The finite element analysis of “plane-strain” tension sample in the elastic region indicates that the stress biaxiality ratio across the gauge width decreases from 0.57 near the mid-point between the two notches to 0 (uniaxial tension) near the notch. While most of the specimen deforms elastically, a small plastic zone may be created near the notch under the loading conditions obtained in this study.

In order to investigate the stress state effect for stress biaxiality ratios greater than 0.57, the double edge-notched plane-strain specimen was modified by the addition of two “stress state” holes as shown in Fig. 1c. Under load, the specimen creates a region of near-equibiaxial stress state ($\sigma_1/\sigma_2 \approx 0.83$). Fig. 2 shows the results of finite element calculation of the stress state in the near-equibiaxial tension sample, in terms of the principal stress distributions along both the gauge width and the gauge length when an average gauge section stress of 210 MPa is applied. The notches and the holes produce a range of multiaxial stress states that vary with location within a sample under load. Specifically, a near equibiaxial stress state of ≈0.83 is achieved at the center of the specimen sample; see Fig. 2c. A similar high degree of stress biaxiality is also computed along a line between the centers of the stress state holes as shown in Fig. 2d. In addition, Fig. 2b shows that there is an extensive region near the center of the gauge section in which the major principal stress is nearly constant while the minor principal stress is decreasing, resulting in a range of stress states that depend on specimen location.[2]

[2] Note that for these plane-stress analyses, the minimum principal stress is always the through-thickness stress, which has a value of zero, and thus we adopt the notation for the in-plane stresses as the “major” and “minor” stresses; both are principal stresses and the major stress is also the maximum principal stress.

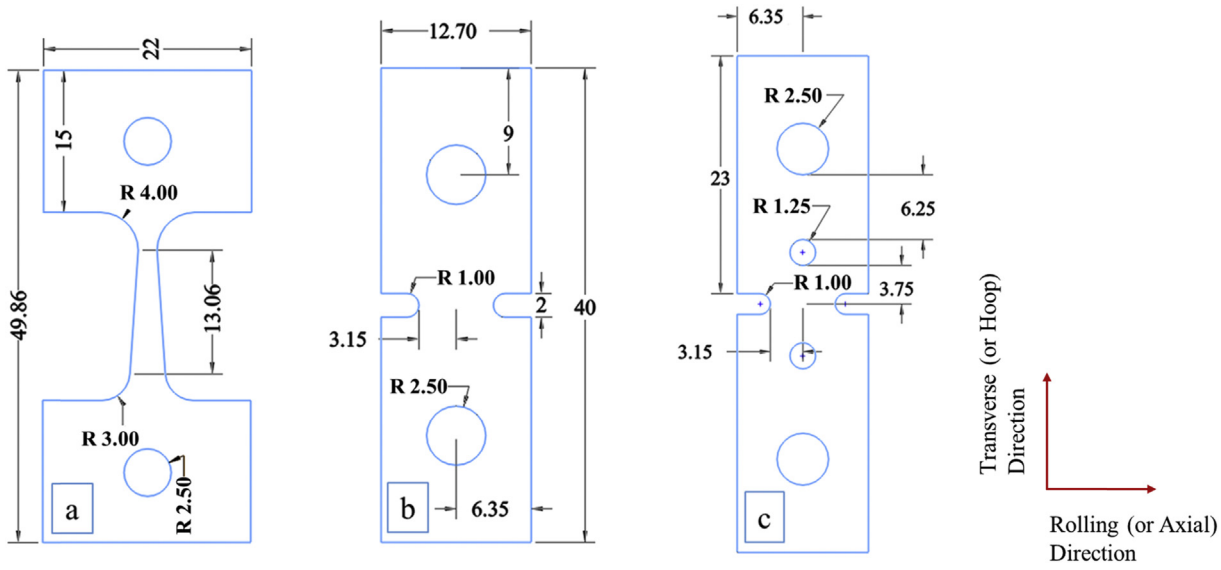

Fig. 1. Specimen geometries: (a) tapered uniaxial tension, (b) "plane-strain tension", and (c) "near-equibiaxial" tension. All dimensions are in "mm".

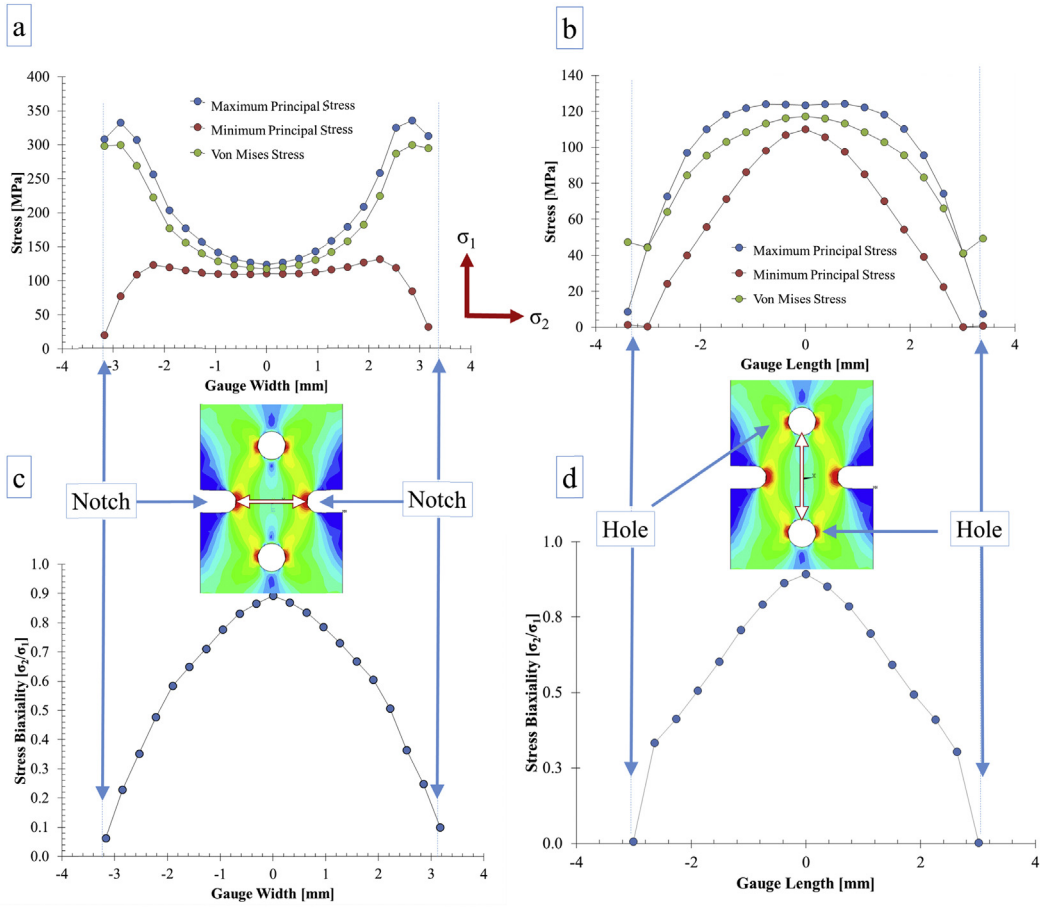

Fig. 2. Calculated mechanical response of the "near-equibiaxial" sample at 400 °C when the average tensile stress across the gauge width (from one notch root to the other) is 210 MPa. In (a) and (b), the major and minor principal stress distributions and the equivalent stress distribution are shown, while in (c) and (d), the stress biaxiality ratio along the gauge width and gauge length are shown. The gauge width is defined from notch root to notch root, and the gauge length is defined as the distance from the edge of one hole to the other.

All specimens were subjected to the two-cycle thermo-mechanical treatment shown in Fig. 3. Uniformly hydrided specimens (≈180 wt ppm hydrogen) were heated to 450 °C (at which temperature the terminal solid solubility of hydrogen dissolution is 267 wt ppm) at a rate of 5 °C/min in order to dissolve the hydrides into the Zircaloy-4 matrix [1]. To homogenize the hydrogen distribution, the samples were kept at 450 °C for 1 h, and then cooled to 150 °C at a cooling rate of 1 °C/min. In order to initiate *out-of-*

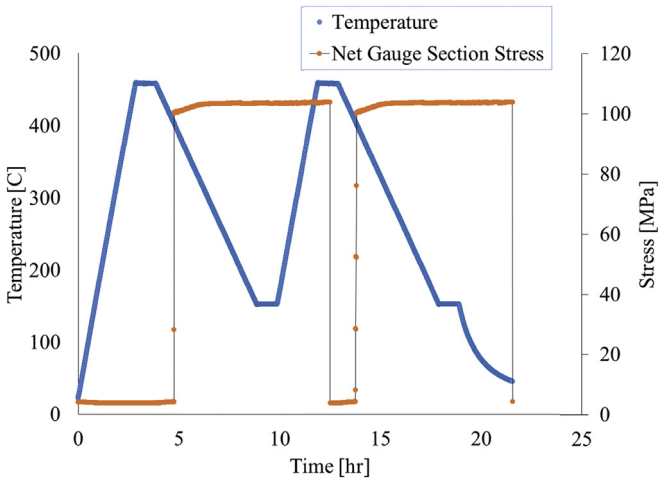

Fig. 3. The thermo-mechanical treatment used: the maximum temperature is 450v°C, the heating rate is 5 °C/min, and the cooling rate is 1 °C/min. In this illustration, the stress across the gauge width for this particular sample was 105 MPa.

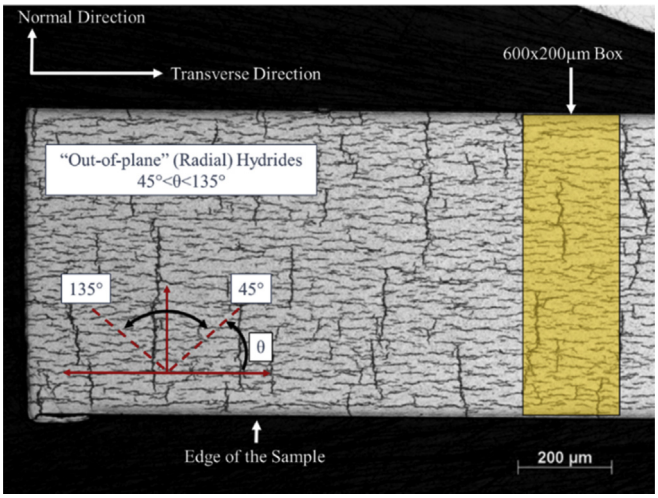

Fig. 4. An optical micrograph illustrating the "through-thickness" hydride microstructure showing a mixture of in-plane and out-of-plane hydrides and a 600 × 200 μm^2 rectangular region used as a basis for determining the out-of-plane hydride fraction.

plane "radial" hydride precipitation (hydride reorientation), a tensile stress was applied to the samples during cool down when the temperature reached 400 °C, i.e. while all hydrogen was still in solution. The applied tensile stress was kept constant upon further cooling down to 150 °C in this study. This is a more penalizing condition than could be expected during vacuum drying as the decreasing gas pressure during cooling would reduce the applied stress. The heat-up, dwell at 450 °C, cool-down under stress below 400 °C, and dwell at 150 °C constituted one thermo-mechanical cycle. Samples were then prepared and examined for metallography.

Samples were examined after swab etching with a solution of 10 HNO_3, 10 H_2O and 1 HF to reveal the hydrides. The hydride microstructure was characterized from optical micrographs of either the "normal" plane showing the flat sheet surface or the "through-thickness" plane that shows the sheet edge parallel to the load direction. For "through-thickness" micrographs, the radial hydride fraction (RHF) used as a metric to evaluate the degree of hydride reorientation was performed on the basis of a 600 × 200 μm^2 rectangular region as the ratio of total length of radially oriented hydrides to the total length of all hydrides, as described in Equation (1) [23,32].

$$\mathrm{RHF} = \frac{\text{Total length of hydrides oriented within } 45^\circ \le \theta \le 135^\circ}{\text{Total length of hydrides at any orientation}} \quad (1)$$

where θ is the angular deviation from the specimen edge, as shown in Fig. 4. The determination of the RHF includes labeling the hydrides, as well as recording the lengths, and the angles of the individual hydride particles. For micrographs that view the "normal" or sheet surface plane, the "in-plane" hydrides in Fig. 4 are oriented parallel to the plane of view, and therefore they are not observable in these micrographs. However, the "out-of-plane" hydrides which are perpendicular to the sheet surface can be clearly seen. Thus, the threshold stresses for hydride reorientation were determined at locations where the in-plane to out-of-plane transition occurs as shown in Fig. 6.

The hydride reorientation threshold stress was determined from optical micrographs of "normal" and "through-thickness" micrographs of samples with nominally 180 wt ppm hydrogen and after the two-cycle thermo-mechanical treatment. For "through-thickness" micrographs, the onset of hydride reorientation was defined as corresponding to a radial hydride fraction of 0.05. For "normal" micrographs where in-plane hydrides are not observed when viewing the sheet surface, the threshold stresses for out-of-plane hydrides were determined by finite element analyses of the maximum principal stress (as well as the minor principal stress) at locations where the out-of-plane hydrides were observed in the micrographs. The accuracy of the "normal face view" of the transition from mainly "in-plane" and to "out-of-plane" hydrides was verified by performing metallography on both the normal face and the edge faces of a tapered uniaxial tensile specimen in locations where a transition to out-of-plane hydrides occurred. Both views showed the hydride reorientation occurred at the same specimen location; thus this metallographic technique did not affect the subsequent value of the threshold stress for hydride reorientation.

The tapered uniaxial tension sample in Fig. 1 enabled a straightforward determination of the threshold stress for hydride reorientation under a uniaxial state of stress by correlating the hydride microstructure from optical micrographs with the local value of the tensile stress along the specimen length. To investigate the effect of stress states with a higher degree of biaxiality on the threshold stress, double-edge notched specimens inducing stress biaxialities in the range of uniaxial tension ($\sigma_2/\sigma_1 = 0$) to near-equibiaxial tension ($\sigma_2/\sigma_1 = 0.8$) within the specimens were utilized. These specimens require the use of finite element analysis to identify the stress states at locations within these specimens and metallography to characterize the hydride microstructure at the same location. Threshold stresses for a range of multiaxial stresses can then be determined using this procedure.

3. The effect of stress biaxiality on the zirconium hydride reorientation

Fig. 5 shows the evolution of hydride microstructure from in-plane hydrides to out-of-plane hydrides in a tapered uniaxial tension sample after the thermo-mechanical treatment in Fig. 3. Because of the taper, the tensile stresses varied along the length of the sample during cooling from high temperature under applied stress, which caused hydride reorientation to occur at a specific locations as shown in Fig. 5. The transition from "in-plane" to "out-of-plane" hydrides occurred at a tensile stress of about 155 MPa

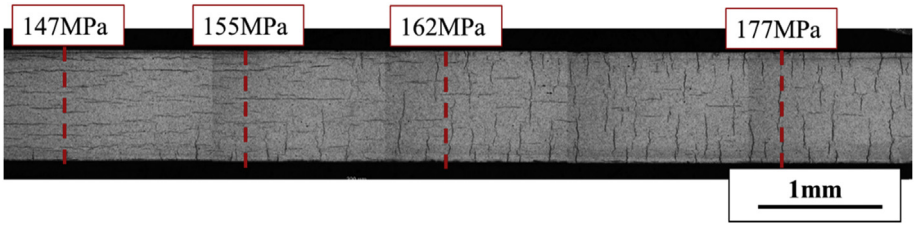

Fig. 5. Hydride microstructure shown in a cross section of a tapered uniaxial tension sample along its edge plane after the two-cycle thermo-mechanical treatment. The threshold stress for hydride reorientation is approximately 155 MPa.

along the length of the tapered specimen. Above 177 MPa, the radial hydride fraction approached one, whereas it was equal to zero at stress levels below 145 MPa. An analysis of this specimen and other tapered samples indicated that for the Zircaloy-4 material used in this study, the threshold stress for hydride reorientation under a uniaxial tension stress state is 155 ± 10 MPa.

Hydride reorientation behavior under multiaxial stress states ($\sigma_2/\sigma_1 > 0$) was assessed using a combination of metallographic examination of double-edge notched tension ("plane-strain" as well as "near-equibiaxial") specimens and finite element analysis of the test geometry. Fig. 6 a shows a hydrided "plane-strain" tension sample after thermo-mechanical treatment and etching to reveal hydrides. The region shown is near the notch and reoriented hydrides can be seen at specific locations. Because both principal stress level and stress biaxiality ratio change throughout the sample, finite element analysis is needed to match the transition points with the local stress level and local stress state. Finite element calculation (see Fig. 6a) show that the stress biaxiality ratio near the notch was equal to 0 (uniaxial tension) and increased rapidly with distance from the notch to $\sigma_2/\sigma_1 = 0.57$ near the center of the gauge section. At other locations, such as near the notch but above or below the minimum width section as illustrated in Fig. 6b, the state of stress is near uniaxial tension ($\sigma_1 > 0$ and $\sigma_2 = 0$). By identifying exact locations from FEA with $\sigma_2/\sigma_1 = 0$, we can again determine the uniaxial tension threshold stress. A similar determination in the region where $\sigma_2/\sigma_1 = 0.57$ yields a plane-strain threshold stress of 110 MPa as shown in Fig. 6c. The determination of threshold stress under near-equibiaxial tension is shown in Fig. 7. Note that the magnitude of the principal and the minor stresses calculated by FEA are indicated by the arrows in Fig. 7. Thus, as shown in Figs. 6 and 7, the threshold stresses for hydride reorientation under varying degrees of stress biaxiality were determined from individual specimens by identifying the locations where the out-of-plane (radial) hydrides are first observed and calculating the corresponding stresses and stress biaxiality ratios at that location for a given load. This procedure was applied to all double-edge notched samples of "plane-strain" and "near-equibiaxial" tension samples. For these specimen geometries, the noticeable features of the out-of-plane hydrides were visible in this field of view over wide regions of the sample, as shown in Fig. 7.

Careful examination of images such as shown in Figs. 6 and 7 shows a marked trend in the dependence of the threshold stress for hydride reorientation on the degree of stress biaxiality. The examination of regions within double edge-notched specimens where uniaxial tension exists, such as in Fig. 6b along the strip of material near the edge of the sample, confirms the value of 155 MPa for the threshold stress previously determined from tapered uniaxial tension specimens for this stress state. In contrast, an examination of the out-of-plane hydride microstructures near the center of the plane-strain specimens such as Fig. 6c shows that the threshold stress for hydride reorientation at this location (where $\sigma_2/\sigma_1 = 0.57$) is only ≈ 110 MPa, significantly lower than the threshold stress of 155 MPa determined for uniaxial tension.

Finally, an examination of the equibiaxial samples such as shown in Fig. 7 shows that the threshold stress for the region where $\sigma_2/\sigma_1 = 0.83$ is only 75 MPa. (The absence of radial hydrides near the specimen edge is consistent with the uniaxial stress state at that location where the local σ_1 value is less than 155 MPa) The 75 MPa value of the threshold stress in near equibiaxial tension is significantly lower than the value of 110 MPa for the threshold stress in near plane strain tension when $\sigma_2/\sigma_1 = 0.57$. Thus, the threshold stress for radial hydride precipitation decreases from 110 MPa to ≈75 MPa as the stress biaxiality ratio increases from 0.5 to 0.83. The consistent trend of these data is that increasing stress biaxiality decreases the threshold stress for hydride reorientation. In all cases, the radial hydrides are oriented normal to the local maximum principal stress direction, as shown in the superposition of micrograph and arrows in Fig. 7.

The overall effect of the stress biaxiality on the threshold stress for hydride reorientation is shown in the Fig. 8 where the threshold stress (as determined by the maximum principal stress) is plotted versus the stress biaxiality ratio. Data from uniaxial sample tests is shown in squares, from plane-strain samples in triangles, and from near-equibiaxial samples in circles. Different colors indicate different individual samples, and different colors in the Fig. 8 indicate different tests. Because a range of stress is present in the higher stress biaxiality samples, it is possible to have triangles or circles with $\sigma_2/\sigma_1 = 0$, i.e. uniaxial tension regions within the plane-strain and the near-equibiaxial tension samples. For the tapered uniaxial tension sample and for the selected regions within the double edge-notched tensile specimens where $\sigma_1/\sigma_2 = 0$, the average threshold stress at locations is 155 ± 10 MPa.

The good agreement in the threshold stress-values under uniaxial tension for all types of samples supports the validity of the data obtained from double edge notched samples. In the literature, the threshold stress for hydride reorientation in CWSR Zircaloy-4 samples subjected to uniaxial tension is reported to be in the range of 140–200 MPa [20,24] with the exception of Daum et al. who observed a value of 85 MPa [19]. For example, Bai et al. determined the threshold stress for plate samples as 150 MPa when the hydrogen content was 1120 wt ppm [20] but for these high hydrogen contents, the hydrides are not completely dissolved at high temperatures, so hydride precipitation initiates in a Zircaloy-4 matrix that already has in-plane hydrides. Colas et al. also observed threshold stresses in the range of 160–200 MPa using sheet samples subjected to uniaxial tension and hydrogen contents of ≈200 wt ppm [24], and Kese reports the threshold stress to reorient hydrides in the range of 140–160 MPa for ring stretch experiments of Zircaloy tube samples under uniaxial tension [23]. Thus, the threshold stress values for uniaxial tension obtained in this study are in the range of most previous measurements.

For the case of near plane-strain tension, the value of the threshold stress for a stress biaxiality ratio of $\sigma_2/\sigma_1 = 0.57$ is 110 ± 7 MPa. This stress biaxiality ratio is close to that present in

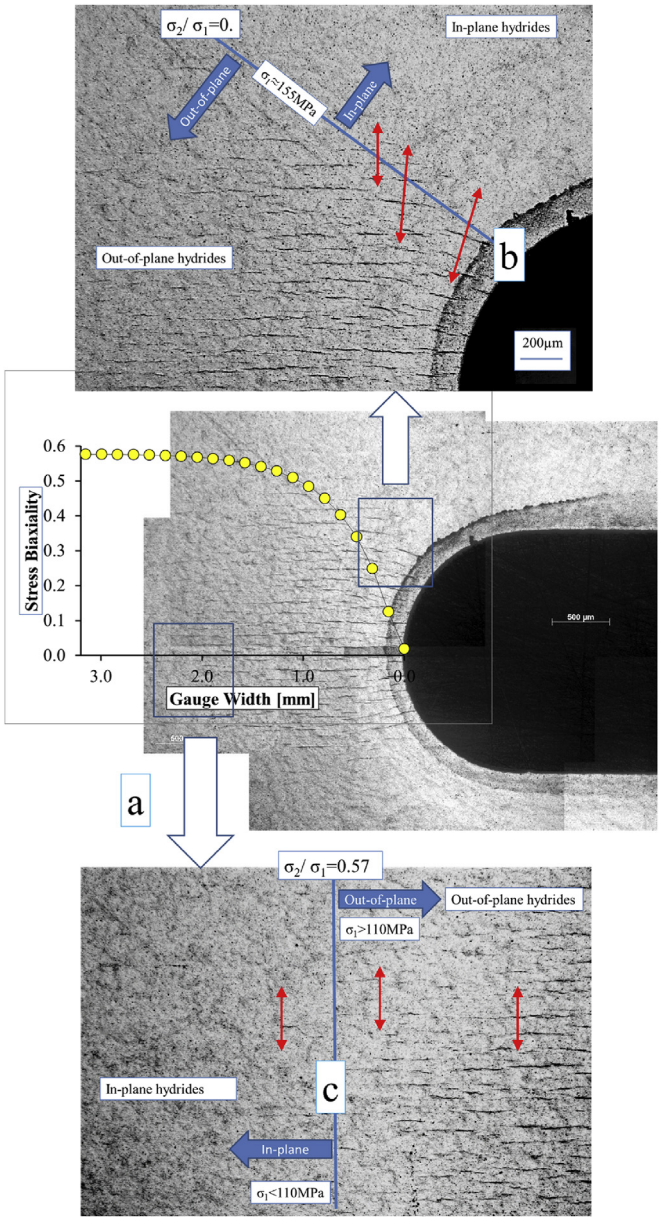

Fig. 6. Optical micrographs showing the out-of-plane hydride microstructure within a double edge notched "plane-strain" tensile specimen. (a) The radial hydride microstructure and stress biaxiality ratio (σ_2/σ_1) across the gauge section. At the applied stress used in this test, out-of-plane hydrides are visible in the uniaxial tensile region near the notch where the local value of the maximum principal stress exceeds 155 MPa as shown in (b). At a stress biaxiality ratio of 0.57, the transition from in-plane to out-of-plane hydrides occurs at maximum principal stress of 110 MPa as shown in (c). The red arrows in (b) and (c) show the orientation of major principal stress direction at those locations. (For interpretation of the references to color in this figure legend, the reader is referred to the web version of this article.)

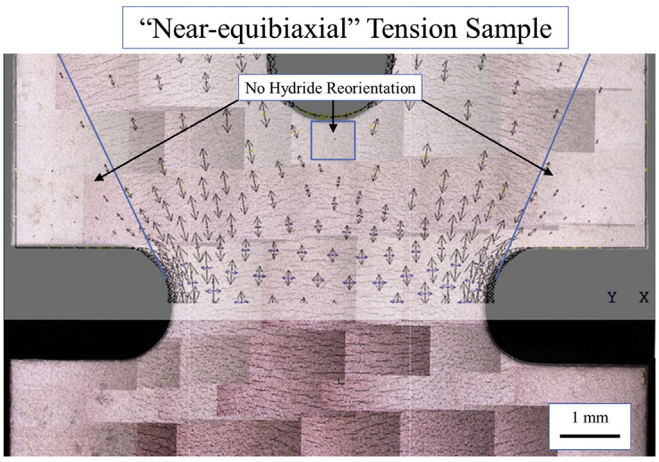

Fig. 7. Optical micrograph showing the hydride microstructure within a "near-equibiaxial" tension sample. The arrows show the major and minor principal stress directions prevalent when a far-field stress is applied.

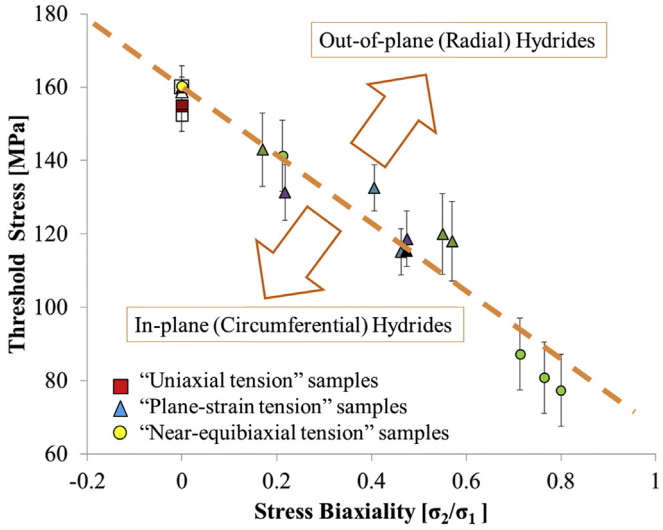

Fig. 8. The threshold stress (major principal stress) for the onset of out-of-plane hydride formation as a function of stress biaxiality. The specimens contained ≈180 wt ppm of hydrogen and were subjected to a two-cycle thermo-mechanical treatment with a maximum temperature of 450 °C as described in the text. Each data point represents the average of 3–5 measurements.

closed end, thin wall internally pressurized tubes ($\sigma_2/\sigma_1 = 0.50$); in the literature, the threshold stresses for internally pressurized tube samples tested under similar conditions range from 70 to 115 MPa [13,15]. Thus, the threshold stress of 110 MPa in this study is at the high limit of previously reported unirradiated internally pressurized tube test data.

In summary, the combination of uniaxial and multiaxial tension test data in Fig. 8 indicates that out-of-plane, (radial) hydride precipitation is enhanced by the presence of a multiaxial stress state. Specifically, the minimum principal stress required for hydride reorientation decreases in a roughly linear manner with increasing stress biaxiality ratio. The effect of increasing stress biaxiality ratio on the threshold stress is significant, with the threshold stress decreasing from ≈155 MPa at $\sigma_2/\sigma_1 = 0$ to ≈75 MPa at $\sigma_2/\sigma_1 = 0.8$, or a decrease of the threshold stress for hydride reorientation by about a factor of two.

The cause of the effect of stress state on the threshold stress is not understood. It is tempting to analyze the effect by applying existing models that predict the critical energy for the nucleation of radial-type hydrides under an external stress field [36–38]. As has been pointed out by this manuscript's reviewer, the difficulty with applying these analyses is that if the in-plane and out-of-plane hydrides are viewed macroscopically as platelets, increasing the stress biaxiality ratio results in the addition of a minor stress (σ_2) that is aligned within the plane of the hydride plate for *both* in-plane and out-of-plane hydrides. Thus, the presence of the minor stress should affect the nucleation of in-plane hydrides in a manner similar to that of out-of-plane hydrides, and no effect of stress state would be expected on the threshold stress, which is contrary to Fig. 8.

Finally, the onset hydride reorientation has been defined by a threshold stress that takes the form of the maximum principal stress. On the other hand, the data in Fig. 8 roughly obey a critical hydrostatic stress ($\sigma_H = 1/3(\sigma_1 + \sigma_2)$ for plane stress) criterion such that $\sigma_H = 51 \pm 7$ MPa at the onset of reorientation. The near constant hydrostatic stress across stress states at the onset of hydride reorientation does suggest that preferential hydrogen accumulation to regions of high stress biaxiality should *not* occur. However, whether such a criterion has a physical basis for the onset of hydride reorientation is not known.

4. Conclusions

In order to examine the effect of stress state on hydride reorientation in Zircaloy-4, tensile tests were performed using sheet specimens that create a variety of stress states ranging from uniaxial to near equibiaxial tension. Matching the stress state calculated by finite element analysis at a specific location within a specimen to the hydride microstructure at that location enabled the determination of the effect of stress state on the threshold stress for hydride reorientation.

The major conclusion of this study is that the presence of a minor principal stress enhances the effectiveness of the major principal stress to initiate hydride reorientation. The experimental results show that as the stress biaxiality ratio increased, the threshold stress for hydride reorientation decreased. The threshold stress was determined to be 155 MPa for uniaxial tension, 110 MPa for "plane-strain" tension, and only 75 MPa for "near-equibiaxial" tension. Significantly, high stress biaxiality conditions close to plane-strain tension may exist in processes like vacuum-drying of nuclear fuel rods.

Acknowledgments

This research was funded by the Nuclear Regulatory Commission (NRC Contract 04-10-156), under the supervision of Harold Scott, and the authors are grateful for this support. We acknowledge helpful discussion with Michael Billone from Argonne National Laboratory. The thorough and insightful comments of Manfred Puls were especially appreciated. The research for this publication was supported by the Pennsylvania State University Materials Research Institute Nano Fabrication Network and the National Science Foundation Cooperative Agreement No. 0335765, National Nanotechnology Infrastructure Network with Cornell University.

References

[1] J.J. Kearns, Terminal solubility and partitioning of hydrogen in the alpha phase of zirconium, Zircaloy-2 and Zircaloy-4, J. Nucl. Mater. 22 (1967) 292–303.
[2] A. McMinn, E.C. Darby, J.S. Schofield, The terminal solid solubility of hydrogen in zirconium alloys, in: G.P. Sabol, J. Moan (Eds.), Zircon. Nucl. Ind. Twelfth Int. Symp. ASTM STP 1354, pp. 173–195.
[3] J.J. Kearns, C.R. Woods, Effect of texture, grain size and cold work on the

precipitation of oriented hydrides in Zircaloy tubing and plate, J. Nucl. Mater. 20 (1966) 241–261.
[4] M.R. Louthan Jr., R.P. Marshall, Control of hydride orientation in zircaloy, J. Nucl. Mater. 9 (1963) 170–184.
[5] C.E. Ells, Hydride precipitates in zirconium alloys (A review), J. Nucl. Mater. 28 (1968) 129–151.
[6] D. Hardie, M.W. Shanahan, Stress reorientation of hydrides in zirconium–2.5% niobium, J. Nucl. Mater. 55 (1975) 1–13.
[7] K. Sakamoto, M. Nakatsuka, Stress reorientation of hydrides in recrystallized Zircaloy-2 sheet, J. Nucl. Sci. Technol. 43 (2006) 1136–1141.
[8] N.A.P. Kiran Kumar, J.A. Szpunar, Z. He, Preferential precipitation of hydrides in textured zircaloy-4 sheets, J. Nucl. Mater. 403 (2010) 101–107.
[9] R.P. Marshall, Control of hydride orientation in zircaloy by fabrication practice, J. Nucl. Mater. 24 (1967) 49–59.
[10] R.P. Marshall, Influence of fabrication history on stress-oriented hydrides in zircaloy tubing, J. Nucl. Mater. 24 (1967) 34–48.
[11] J. Desquines, D. Drouan, M. Billone, M.P. Puls, P. March, S. Fourgeaud, et al., Influence of temperature and hydrogen content on stress-induced radial hydride precipitation in Zircaloy-4 cladding, J. Nucl. Mater. 453 (2014) 131–150.
[12] A.M. Alam, C. Hellwig, Cladding tube deformation test for stress reorientation of hydrides, J. ASTM Int. 5 (2008). Paper ID JAI101110.
[13] M. Aomi, T. Baba, T. Miyashita, K. Kamimura, T. Yasuda, Y. Shinohara, et al., Evaluation of hydride reorientation behavior and mechanical properties for high-burnup fuel-cladding tubes in interim dry storage, J. ASTM Int. 5 (2008). Paper ID JAI101262.
[14] M. Billone, T. Burtseva, R. Einziger, Ductile-to-brittle transition temperature for high-burnup cladding alloys exposed to simulated drying-storage conditions, J. Nucl. Mater. 433 (2013) 431–448.
[15] H.C. Chu, S.K. Wu, R.C. Kuo, Hydride reorientation in Zircaloy-4 cladding, J. Nucl. Mater. 373 (2008) 319–327.
[16] R.N. Singh, R. Lala Mikin, G.K. Dey, D.N. Sah, I.S. Batra, P. Ståhle, Influence of temperature on threshold stress for reorientation of hydrides and residual stress variation across thickness of Zr–2.5Nb alloy pressure tube, J. Nucl. Mater. 359 (2006) 208–219.
[17] H.-J. Cha, J.-J. Won, K.-N. Jang, J.-H. An, K.-T. Kim, Tensile hoop stress-, hydrogen content- and cooling rate-dependent hydride reorientation behaviors of Zr alloy cladding tubes, J. Nucl. Mater. 464 (2015) 53–60.
[18] K.B. Colas, A.T. Motta, M.R. Daymond, M. Kerr, J.D. Almer, P. Barberis, et al., Hydride platelet reorientation in zircaloy studied with synchrotron radiation diffraction, J. ASTM Int. 8 (2011) 103033.
[19] R.S. Daum, S. Majumdar, Y.Y. Liu, M.C. Billone, Radial-hydride embrittlement of high-burnup Zircaloy-4 fuel cladding, J. Nucl. Sci. Technol. 43 (2006) 1054–1067.
[20] J.B. Bai, N. Ji, D. Gilbon, C. Prioul, D. Francois, Hydride embrittlement in Zircaloy-4 plate. Part II: interaction between the tensile stress and hydride morphology, Metall. Mater. Trans. A 25A (1994) 1199–1208.
[21] D. Hardie, M.W. Shanahan, The effect of residual stresses on hydride orientation in a zirconium-2.5% niobium alloy, J. Nucl. Mater. 50 (1974) 40–46.
[22] R.N. Singh, R. Kishore, S.S. Singh, T.K. Sinha, B.P. Kashyap, Stress-reorientation of hydrides and hydride embrittlement of Zr-2.5 wt% Nb pressure tube alloy, J. Nucl. Mater. 325 (2004) 26–33.
[23] K. Kese, Hydride Re-orientation in Zircaloy and Its Effect on the Tensile Properties, Department of Materials Science and Engineering, Royal Institute of Technology, Stockholm, Sweden, 1998.
[24] K.B. Colas, A.T. Motta, M.R. Daymond, J.D. Almer, Effect of thermo-mechanical cycling on zirconium hydride reorientation studied in situ with synchrotron X-ray diffraction, J. Nucl. Mater. 440 (2013) 586–595.
[25] J. Desquines, D.A. Koss, A.T. Motta, B. Cazalis, M. Petit, The issue of stress state during mechanical tests to assess cladding performance during a reactivity-initiated accident (RIA), J. Nucl. Mater. 412 (2011) 250–267.
[26] O.N. Pierron, D.A. Koss, A.T. Motta, K.S. Chan, The influence of hydride blisters on the fracture of Zircaloy-4, J. Nucl. Mater. 322 (2003) 21–35.
[27] P. Delobelle, P. Robinet, P. Geyer, P. Bouffioux, A model to describe the anisotropic viscoplastic behaviour of Zircaloy-4 tubes, J. Nucl. Mater. 238 (1996) 135–162.
[28] P.A. Raynaud, D.A. Koss, A.T. Motta, Crack growth in the through-thickness direction of hydrided thin-wall Zircaloy sheet, J. Nucl. Mater. 420 (2011) 69–82.
[29] E. Tenckhoff, Review of deformation mechanisms, texture, and mechanical anisotropy in Zirconium and Zirconium base alloys, ASTM Spec. Tech. Publ. 1467 (2005) 25–50.
[30] O.N. Pierron, D.A. Koss, A.T. Motta, Tensile specimen geometry and the constitutive behavior of Zircaloy-4, J. Nucl. Mater. 312 (2003) 257–261.
[31] T.M. Link, D.A. Koss, A.T. Motta, Failure of Zircaloy cladding under transverse plane-strain deformation, Nucl. Eng. Des. 186 (1998) 379–394.
[32] M.E. Flanagan, The effect of hydrogen on the deformation behavior of Zircaloy-4, in: Proc. 2008 Water React. Fuel Perform. Meet, Penn State University, Seoul, Korea, 2008.
[33] A. Glendening, D.A. Koss, A.T. Motta, O.N. Pierron, R.S. Daum, Failure of hydrided Zircaloy-4 under equal-biaxial and plane-strain tensile deformation, J. ASTM Int. 2 (2005) paper ID12441.
[34] P. Raynaud, D.A. Koss, A.T. Motta, K.S. Chan, Fracture toughness of hydrided Zircaloy-4 sheet under through-thickness crack growth conditions, in: B. Kammenzind, M. Limbäck (Eds.), Fifteenth Int. Symp. Zr Nucl. Ind 1505, ASTM STP, 2007, pp. 163–177.
[35] L.J. Siefken, E.W. Coryell, E.A. Harvego, J.K. Hohorst, Matpro - a library of materials properties for light-water-reactor accident analysis, in: SCDAP/RELAP5/MOD 3.3 Code Manual, Vol. 4, 2001. Rev. 2.
[36] C.E. Ells, The stress orientation of hydride in zirconium alloys, J. Nucl. Mater. 35 (1970) 306–315.
[37] M.P. Puls, Hydrogen induced delayed cracking: 2. effect of stress on nucleation, growth, and coarsening of zirconium hydride precipitates, Aecl 8381 (1984) 30.
[38] W. Qin, N.A.P. Kiran Kumar, J.A. Szpunar, J. Kozinski, Intergranular δ-hydride nucleation and orientation in zirconium alloys, Acta Mater. 59 (2011) 7010–7021.